Fracture path in an anisotropic material in the light of a friction experiment

David Chateau, Jean-Christophe Géminard

Fracture path in an anisotropic material in the light of a friction experiment.

D. Chateau and J.-C. Géminard*
Laboratoire de Physique, Ecole Normale Supérieure de Lyon, CNRS, Université de Lyon, 46 Allée d´Italie, 69364 Lyon Cedex, France

A slider is pulled by means of a flexible link on a flat solid surface which exhibits anisotropic frictional properties. The resulting trajectory of the slider is assessed experimentally. First, we check that the experimental results are in excellent agreement with a theoretical description of the problem based on an expression of the frictional forces. Second, we point out that the trajectory of the slider can be recovered by the use of a "maximum of energy release rate" criterion which is generally used to predict the path of a fracture even if the validity of the principle is difficult to verify in the latter complex systems.

PACS numbers: 46.90.+s; 62.20.Qp; 46.50.+a; 83.60.Uv

I. INTRODUCTION

Fractures are ubiquitous in everyday life. Examples range, from the harmless, annoying but maybe useful, craquelures on paintings [1, 2] to the dramatic rupture of large structures such as aircraft fuselages [3]. Because of its high practical importance, fracture mechanics developed dramatically as an engineering discipline during the last century. The seminal works of Griffith [4], and later Irwin and Orowan [5, 6], have provided the standard tools to explain fracture in engineered structures. Criterions were proposed for the threshold and direction of fracturing. In the present article, we shall focus on, specifically, the potential applicability of a "maximum energy release rate" criterion [7] when anisotropy of the material properties comes into play.

One of the most important questions raised by the fracturing process, apart from the location of the nucleation sites and threshold, is the direction in which the fracture will propagate. Nice examples are provided by experiments performed in thin sheets. They reveal that the direction can be tuned by the boundary conditions [8–10], or in other words by the geometry of the stress field. In the same way, fractures interact through the stress field and, for instance, the tearing of a rectangular flap from a sheet leaves generally a convergent tear, the cortina mode [11, 12]. But in a stretched foil, provided that the physical properties of the material are isotropic, an isolated fracture propagates perpendicularly to the stretching direction, which can be easily understood from simple symmetry arguments.

When the anisotropy of the material properties comes into play, simple symmetry arguments are not relevant to account for the fracturing direction which is not necessarily perpendicular to the direction of the maximum stretching stress, as illustrated in thin sheets [13]. A very striking illustration is provided by the trajectory of a crack forced to propagate in a thin sheet of brittle material by means of a rod, namely a blunt object [14]. If the material is isotropic, the fracture trajectory is a spiral which does not depend on the details of the rod trajectory. If the material is anisotropic, the trajectory exhibits oscillations around the spiral and, even, almost straight segments and kinks if the anisotropy is large. In order to account for the trajectory, one could use possible generalizations of the symmetry criterion to the case where fracture energy depends on the orientation that were proposed rather recently [15–18], but are not widely accepted by the fracture community, and the authors do prefer to consider the "maximum of energy release rate" criterion [7] which, however, must be considered with caution.

Inspired by the latter experiment, in particular by the appearance of straight segments and kinks which reminded us of facets and angular points in equilibrium shapes of crystals, we sought for a system permitting the observation of closed trajectories. One would thus wonder if the trajectory would not relate to the dependence of the fracture energy on the orientation as the equilibrium shape of a crystal relates to the dependence of the surface free energy on the cristallographic orientation [19, 20]. The impossibility to make a fracture follow a periodic and closed trajectory led us to consider a frictional system instead.

At this point, it is particularly interesting to underline common features of fracturing and friction processes [21]. The parallel between friction and fracture has already been drawn successfully so as to formulate friction theories, based on microscopic considerations, using concepts developped to describe fracture [22]. Here, we draw the parallel between fracture and friction at the macroscopic scale. The propagation of a fracture leads to the creation of two new surfaces and the associated energetic cost increases linearly with the fracture length, whereas elastic energy loaded in the material is released. Similarly, when a slider is pulled by means of a spring on a flat substrate, the energy dissipated by friction increases linearly with the sliding distance, whereas elastic energy loaded in the spring is released [23].

The similarities between the fracturing and friction processes are such that one can hope to get insights in the mechanisms governing the fracture paths from a fric-

* jean-christophe.geminard@ens-lyon.fr

tion experiment. Interestingly, in the friction problem, the elastic contribution reduces to the elongation of the spring whereas, in the fracture problem, the elastic contribution is complicated. For symmetry reasons, if the frictional properties of the substrate are isotropic, the slider moves in the pulling direction. But, if the frictional properties of the substrate are anisotropic [24], the slider does not necessarily move in the pulling direction [25] like a fracture which does not necessarily move perpendicularly to the stretching direction in an anisotropic material. Even more interesting, considering the fracturing process, one could wonder if the anisotropy of the fracture energy governs the fracture trajectory alone or if the anisotropy of the elastic properties of the material also come into play. In the frictional system, the anisotropy of the friction alone is responsible for the anisotropy of the trajectory.

We propose to produce periodic trajectories by pulling one end of the spring along a circle whereas the slider is attached at the other end. The geometrical properties of the trajectories are analyzed with respect to the anisotropy of the frictional properties of the substrate.

II. BASIC CONCEPTS

We consider a material point M (mass m) in frictional contact with a horizontal surface. We assume that the point M is continuously in motion, so that we can consider that the frictional contact between the slider and the surface can be characterized by a unique friction coefficient (*i.e.* the dynamical friction coefficient), $\mu(\alpha)$, that however depends on the sliding direction, α. By definition, for a displacement $\mathbf{t}\,dl$ in the direction α with respect to a frame of reference attached to the surface ($\mathbf{t}$ is the unit tangent vector to the trajectory of M), the amount of energy $\delta W_\mu = \mu(\alpha)\, m\, g\, dl$ is dissipated by friction (g denotes the acceleration due to the gravity).

Let us now consider that the external force $\mathbf{F}$ is applied to the point M (Fig. 1a). The work of $\mathbf{F}$ associated with the displacement $\mathbf{t}\,dl$ is $\delta W = (\mathbf{F}.\mathbf{t})\,dl$. Assuming that the work of the force $\mathbf{F}$ is entirely dissipated by friction, we get $\mathbf{F}.\mathbf{t} = \mu(\alpha)\, m\, g \equiv f(\alpha)$ where, for convenience, we introduced $f(\alpha)$, the frictional force in the direction α. The energy balance thus provides a relation between the applied force, the frictional properties of the contact and the sliding direction, but note that the condition is not sufficient to determine the sliding direction if the frictional contact is anisotropic (Fig. 1b).

We now aim at finding the angle θ that the trajectory makes with the direction of the applied force. We assume that the slider is experiencing a continuous motion (*i.e.* no stick-slip. Indeed, the actual picture would not hold true if the slider came to rest and, thus, the static frictional coefficient came into play [21]). In this framework, $f(\alpha)$ can be regarded as the minimum force to apply in the direction α to make M move in that specific direction. Assuming that the material point moves in the first possible direction, thus as soon as $\mathbf{F}.\mathbf{t}$ reaches the threshold force $f(\alpha)$ in any direction, we get the second condition that the sliding direction is given by the point at which the curves $f(\alpha)$ and $\mathbf{F}.\mathbf{t}$ are tangent (Fig. 1b), which leads to : $\frac{\partial}{\partial\alpha}(\mathbf{F}.\mathbf{t})\Big|_{\mathbf{F}} = f'(\alpha)$. Denoting $\mathbf{n} = \frac{\mathbf{dt}}{\mathbf{d}\alpha}$ the normal to the trajectory , we can write this second condition $\mathbf{F}.\mathbf{n} = f'(\alpha)$.

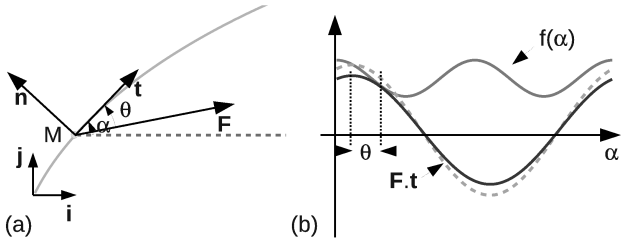

FIG. 1. **Sketch of the considered situation** – (a) The force $\mathbf{F}$ is applied to the material point M. As a result, M moves along the vector $\mathbf{t}$ which makes the angle α with the direction $\mathbf{i}$ of the frame of reference attached to the surface and the angle θ with $\mathbf{F}$. The vector $\mathbf{t}$ is the local tangent to the trajectory (grey line). (b) Frictional force $f(\alpha)$ (light-gray line) and projection $\mathbf{F}.\mathbf{t}$ of the applied force in the sliding direction as a function of α. For a large intensity F of the applied force (dashed line), the energy balance is satisfied for two different sliding directions. The sliding direction is thus uniquely defined only for the specific intensity of the applied force F which makes the curves tangent (dark-grey line).

In summary, the two conditions that $\mathbf{F}.\mathbf{t} = f(\alpha)$ and $\mathbf{F}.\mathbf{n} = f'(\alpha)$ constrain the sliding direction and thus govern the slider trajectory. Taking into account that $\mathbf{F}.\mathbf{t} = \cos\theta$ and $\mathbf{F}.\mathbf{n} = -\sin\theta$, reminding that $f = \mu\, m\, g$, we write the final result:

$$\frac{\mathbf{F}.\mathbf{n}}{\mathbf{F}.\mathbf{t}} = -\tan\theta = \frac{\mu'}{\mu} \qquad (1)$$

where the right member μ'/μ is taken for the sliding direction. In the next section (Sec. III), we describe an experiment which makes it possible to test experimentally that a mass in frictional contact with a surface exhibiting anisotropic friction properties indeed experiences trajectories compatible with Eq. (1).

III. EXPERIMENTS

In order to confront Eq. (1) with the experiment, we chose to force a slider to follow periodic trajectories on a solid surface. The idea is to assess the relation between the friction properties (anisotropy, symmetry) and the geometrical properties of the slider trajectory.

The experimental device consists of a melamine wood board (50×50 cm^2, Fig. 2). At the center, the axis of a DC motor, perpendicular to the board plane, drives a metallic arm (length 25 cm) which remains parallel to the board surface (gap about 1 mm). In the range of

accessible voltages (0-12V), the angular velocity ranges from 0 to 4 rpm.

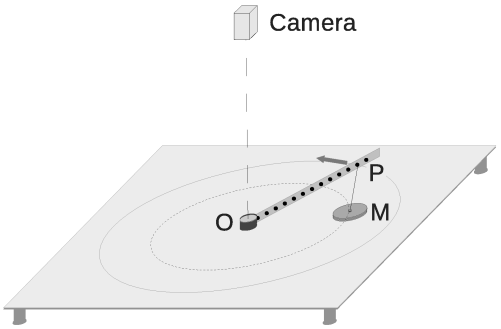

FIG. 2. **Sketch of the experimental device**

The slider consists of a brass disk (thickness 1 cm, diameter 2, 3 or 4 cm). In order to insure reproducible friction properties, the bottom surface of the slider is covered with Bristol board [26].

A link (*i.e.* a thin nylon fishing line) connects the slider to the rotating arm. At one end, in order to insure that it does not apply any significant torque to the slider, the nylon wire makes a loose loop around a lug located at the center M of the top. At the other end, the link is firmly attached to the arm at a point P whose distance OP to the center of rotation can be tuned from 1 to 24 cm by steps of 1 cm.

A digital camera (JAI, CB-080 GE), located 1.8 m at the vertical of the center O, images the system along the symmetry axis. The trajectory of the point M is recorded during several revolutions at 30 images/sec (1024×1024 px^2). The positions $(x_{\rm P}, y_{\rm P})$ and $(x_{\rm M}, y_{\rm M})$ of the points P and M respectively are obtained by subsequent analysis of the movie with ImageJ [27].

IV. EXPERIMENTAL RESULTS

Here, we discuss two experimental cases, the 1-fold and the 2-fold anisotropies, that are described theoretically in appendix A.

Before reporting the results, let us remark that, on the one hand, the link is almost inextensible, which insures that the slider experiences a continuous motion (no stick-slip [23]). On the other hand, we checked that the results are independent of the rotation velocity and, in addition, of the slider diameter. We thus report data obtained with one slider (diameter 3 cm) rotated at 0.5 rpm.

A. 1-fold anisotropy

The first, easy way, to generate an effective anisotropic friction is to tilt the surface. Indeed, denoting β the angle the surface makes with the horizontal, one can immediately check that the energy cost per unit length along the maximum slope is $(\mu_{\rm d}\cos\beta - \sin\beta)\,mg$ for a slider moving downwards and $(\mu_{\rm d}\cos\beta + \sin\beta)\,mg$ for a slider moving upwards, the cost along the perpendicular direction being equal to $\mu_{\rm d}\cos\beta\, mg$. Tilting the surface by an angle β is thus equivalent to an anisotropic surface exhibiting the frictional coefficient $\mu(\alpha) = \mu_0\,(1+\epsilon\,\cos\alpha)$ with $\mu_0 = \mu_{\rm d}\cos\beta$ and $\epsilon = \frac{\tan\beta}{\mu_{\rm d}}$. We can then assess experimentally the anisotropy of the trajectory as a function of the two parameters, the reduced length $l \equiv PM/OP$ and the anisotropy ϵ that can be tuned continuously.

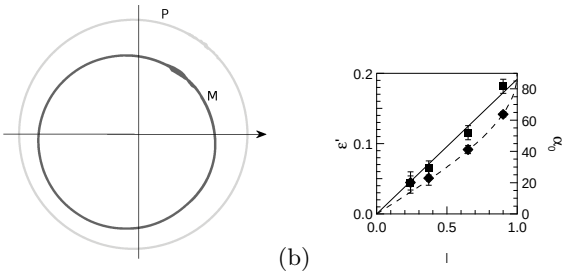

FIG. 3. **1-fold anisotropy** – (a) Trajectories of the points P and M – The arrow indicates the upward slope. Here, we report results obtained for $\beta = 3.2$ deg. We observe that the trajectory of the slider remains almost circular but out-of-center as predicted theoretically (Eq. A.6). (b) Anisotropy ϵ' (squares) and angle α_0 (diamonds) vs. reduced length l. We observe an excellent agreement with the theoretical predictions (continuous and dashed lines, respectively).

Let us first point out that we characterized the effective frictional properties using a force sensor and pulling the slider downwards and upwards. Doing so, we obtained the value of the dynamical frictional coefficient $\mu_{\rm d} = (0.28 \pm 0.01)$ and checked that the dependency of the anisotropy ϵ on the tilt angle β is indeed compatible with the latter value of $\mu_{\rm d}$.

We then contrasted our experimental measurements with the theoretical predictions of Eq. (A.6). We checked that the trajectory of the slider (Fig. 3a) is satisfactorily described by $r(\alpha) = r_0\,[1-\epsilon'\cos(\alpha-\alpha_0)]$ (Eq. A.6). and that the anisotropy of the trajectory ϵ' is indeed proportional to the anisotropy of the friction ϵ in the limit of small anisotropy, thus for small tilt angle β. Then, we assessed the dependency of the anisotropy ϵ' and of the angle α_0 on the reduced length l (Fig. 3b). An excellent agreement is obtained without any adjustable parameter.

B. 2-fold anisotropy

We used a second way to generate an anisotropic friction. The surface of the melamine board is covered with a thin wood board clearly exhibiting rids in a given direction. We checked in this case that the frictional coefficient was the same in both directions along the principal axes and that one could satisfactorily consider a dependency of the frictional coefficient in the form: $\mu(\alpha) = \mu_0\,(1 + \epsilon_2\,\cos 2\alpha)$ with $\epsilon_2 \simeq 3.5\ 10^{-2}$.

In this second case, we observe that the trajectories are almost ellipses, centred in O, correctly described by $r(\alpha) = r_0\,[1 - \epsilon_2'\cos 2(\alpha - \alpha_0)]$ (Eq. A.7). The dependencies of the anisotropy of the trajectory, ϵ_2', and of the angle α_0 are again in good agreement with the theory without any adjustable parameter.

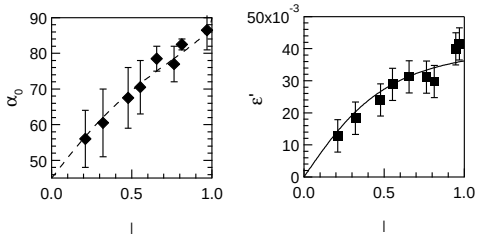

FIG. 4. **2-fold anisotropy** – (a) Angle α_0 vs. reduced length l – The experimental data (diamonds) are in excellent agreement with the theoretical prediction [dashed line, Eq. (A.7); the error bars are obtained from the interpolation of the data]. (b) Anisotropy ϵ' vs. reduced length l – Even if the agreement is not as good as obtained for the angle α_0, the dependency of ϵ' on l if compatible with Eq. (A.7).

Note that the functional dependencies of the anisotropy and angle on the reduced length l differ qualitatively between the 1-fold and 2-fold anisotropies. The agreement between the experimental measurements and the theoretical predictions from Eq. (1) in both cases validates the latter. In the next section, we discuss the possibility to recover the result from an energetic argument.

V. ENERGY RELEASE RATE

Let us first discuss the experimental situation in regards to the "maximum of energy release rate" criterion. To do so, we start by considering an energetic balance. We consider the general situation sketched in the figure 5. The force $\mathbf{F}$ is applied to the material point M of mass m in frictional contact with the surface. As a consequence, the point M is displaced in the direction of $\mathbf{t}$, making the angle θ with the direction of the force $\mathbf{F}$.

Let us consider an elementary work $\delta\mathcal{W}$ of the applied force, associated with a displacement dl^* of M in the direction of $\mathbf{t}$. Taking into account that $\mathbf{t}$ makes the angle θ with $\mathbf{F}$, we can write that the displacement dl of M along $\mathbf{F}$ is $dl = \cos\theta\, dl^*$. The associated work of the friction $\delta\mathcal{W}_\mu = f(\theta)\, dl^*$, where $f = \mu\, m\, g$ is the frictional force and μ the value of the frictional coefficient in the direction of $\mathbf{t}$.

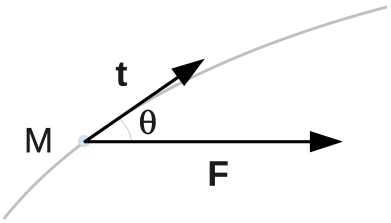

FIG. 5. **Sketch of the considered situation** – The force $\mathbf{F}$ is applied to material point M. As a result, M moves along the vector $\mathbf{t}$ which makes the angle θ with $\mathbf{F}$. The vector $\mathbf{t}$ is the local tangent to the trajectory (grey curve).

Considering that the work $\delta\mathcal{W}$ is either converted in elastic energy $\delta\mathcal{E}$ (for instance in the pulling system) or dissipated by friction, the energy balance can be written:

$$\delta\mathcal{W} = \delta\mathcal{E} + \delta\mathcal{W}_\mu \tag{2}$$

The above energy balance (Eq. 2) makes it possible to write the change in the elastic energy $\delta\mathcal{E} = [F\,\cos\theta - f(\theta)]\, dl^*$ and, finally, the energy release rate:

$$\mathcal{E}_{\rm rr} \equiv -\frac{\partial\mathcal{E}}{\partial l^*}\Big|_F = -F\,\cos\theta + f(\theta). \tag{3}$$

The condition of maximum energy-release rate then writes:

$$\frac{\partial\mathcal{E}_{\rm rr}}{\partial\theta}\Big|_F = F\,\sin\theta + f'(\theta) = 0. \tag{4}$$

Then taking into account that the energy conservation imposes $F\,\cos\theta = f(\theta)$ in the limit of an infinitely stiff driving system [by taking $\delta\mathcal{E} = 0$ in Eq. (2)], and reminding $f = \mu\, m\, g$, we finally write :

$$\tan\theta = -\frac{\mu'}{\mu}. \tag{5}$$

where the second member $-\mu'/\mu$ is taken for the sliding direction. We note that, interestingly, the angle predicted by the latter energetic argument is consistent with the result obtained by considering the force (Sec. II) and validated by the experiment (Sec. IV).

VI. CONCLUSION

We considered the case of a slider in continuous motion. In this case, the friction properties are accounted for by a unique frictional coefficient, independent of the velocity, which however can depend on the direction.

The analogous rupture-problem would concern the quasi-static propagation of a fracture whose energy would not depend on the velocity but, potentially, on the direction. In addition, the displacement of the slider with respect to the surface is only associated with friction and, especially, does not involve any plastic deformation. Thus, the frictional system mimics the fracturing process in an anisotropic, brittle, material.

A first potential extension of the experiment would be to achieve very large anisotropy and thus to produce kinks and facets. An additional question is that of the existence of any geometrical construction, analogue of the Wulff construction [19], to obtain the trajectory from the μ-plot, namely from the representation of the values $\mu(\theta)$ of the frictional coefficient in polar coordinates. Finally, it would be also interesting to analyze the effects of a difference between the static and the dynamical frictional coefficients, when the slider is experiencing a stick-slip motion, which would mimic a fracture propagating by fits and starts.

It remains that we obtained a good agreement between the experimental and theoretical trajectories of a slider pulled on an anisotropic surface. The equations governing the trajectories have been obtained, independently, first by considering the friction force and, second a "maximum of energy release rate" criterion, which indicates that the latter criterion applies in the present experimental situation. Even if the result obviously does not constitutes a proof, it is at least a simple illustration that can be potentially used for educational purpose.

ACKNOWLEDGMENTS

The authors thank D. Le Tourneau for the help provided in the design and setup of the experimental device and J. Bico, F. Melo and B. Roman for fruitful discussions.

Appendix A

In the present appendix, we determine, based on Eq. (1), the trajectories of the slider for the two cases explored experimentally.

Let us consider a material point M pulled thanks to an inextensible, but flexible, link (a thin wire, for instance) attached to a point P which experiences a circular trajectory centred in O (Fig. A.1). We denote R the radius of the circular trajectory of P and a the length of the link MP. The material point M is pulled by the rotation of P around O (the vector $\mathbf{OP}$ makes the angle ω with a reference axis) whereas the link PM is free to rotate in P.

Before considering the anisotropic case, it is interesting to consider the trajectory experienced by the point M when the friction properties are isotropic. In this case,

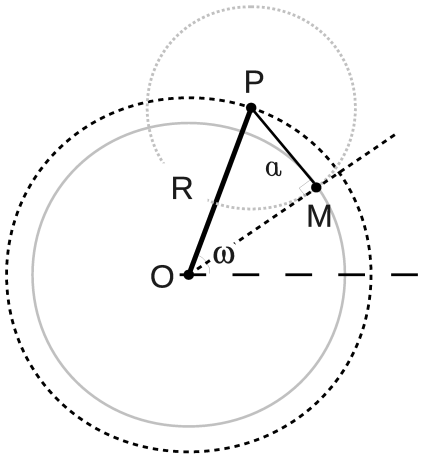

FIG. A.1. **Sketch of the experimental configuration**

because of the symmetry of the problem, one expects the trajectory of M to be a circle (continuous gray line in Fig. A.1). The position of M is obtained by considering that M lies on the circle of center P and radius a (gray dashed line) and that MP must be tangent to the trajectory (indeed, in absence of anisotropy, the slider moves in the direction of the applied force, thus in the direction of the link MP). The last condition imposes that $\widehat{OMP}$ is a right angle and, thus, that (OM) is tangent to the circle of center P and radius a. The trajectory of M is thus a circle of center O and radius r such that $r^2 + a^2 = R^2$, *i.e.* $r = \sqrt{R^2 - a^2}$. Note that accessible configurations are limited to $a \leq R$. Indeed, when the link PM is longer than the radius OP, the material point M tends to rotate around the point P and the link to wrap around the rotation axis in O. The ratio $l \equiv a/R$ is thus the unique control parameter of the problem for the anisotropic case and the next results will be reported as a function of l in the range $[0, 1[$. In the following, we take $R = 1$.

Considering now the anisotropic case, one must determine the trajectory of M taking Eq. (1) into account. To do so, we will describe the position of the point M, for a given angle ω, in the frame $(\mathbf{u}_r, \mathbf{u}_w)$, where $\mathbf{u}_r$ denotes the unit vector such that $\mathbf{OP} = \mathbf{u}_r$ (remember that $R = 1$) and $\mathbf{u}_w$ its normal. We introduce the angle ϕ such that $\mathbf{PM} = l\,(\cos\phi\,\mathbf{u}_r + \sin\phi\,\mathbf{u}_w)$. Obtaining the trajectory of M is equivalent to obtaining the function $\phi(\omega)$.

The local tangent to the trajectory equals (by derivation of $\mathbf{OM}$ with respect to ω):

$$\mathbf{t} = \frac{-l\,(1+\phi')\,\sin\phi\,\mathbf{u}_r + [1 + l\,(1+\phi')\,\cos\phi]\,\mathbf{u}_w}{\sqrt{1 + 2\,l\,(1+\phi')\,\cos\phi + l^2\,(1+\phi')^2}} \tag{A.1}$$

and thus the normal:

$$\mathbf{n} = -\frac{[1 + l\,(1+\phi')\,\cos\phi]\,\mathbf{u}_r + l\,(1+\phi')\,\sin\phi\,\mathbf{u}_w}{\sqrt{1 + 2\,l\,(1+\phi')\,\cos\phi + l^2\,(1+\phi')^2}}. \tag{A.2}$$

The angle that the tangent $\mathbf{t}$ makes with the direction $\mathbf{i}$ attached to the surface is given by:

$$\cos\alpha = \mathbf{t}.\mathbf{i} \tag{A.3}$$
$$= -\frac{l\,(1+\phi')\,\sin\phi\,\cos\omega + [1 + l\,(1+\phi')\,\cos\phi]\,\sin\omega}{\sqrt{1 + 2\,l\,(1+\phi')\,\cos\phi + l^2\,(1+\phi')^2}}$$
$$\sin\alpha = \mathbf{t}.\mathbf{j} \tag{A.4}$$
$$= \frac{-l\,(1+\phi')\,\sin\phi\,\sin\omega + [1 + l\,(1+\phi')\,\cos\phi]\,\cos\omega}{\sqrt{1 + 2\,l\,(1+\phi')\,\cos\phi + l^2\,(1+\phi')^2}}.$$

The differential equation governing the trajectory is obtained by replacing $\mathbf{t}$, $\mathbf{n}$, and α in Eq. (1). Considering that $\mathbf{F}$ and $\mathbf{PM}$ are collinear, the latter equation reduces to $\frac{\mathbf{PM}.\mathbf{n}}{\mathbf{PM}.\mathbf{t}} = \frac{\mu'(\alpha)}{\mu(\alpha)}$:

$$\frac{\cos\phi + l\,(1+\phi')}{\sin\phi} = -\frac{\mu'(\alpha)}{\mu(\alpha)} \tag{A.5}$$

where, we remark, the magnitude of the force $\mathbf{F}$ does not appear. To go farther, one must introduce the dependency of the friction coefficient μ on the angle α. In the next subsections, we consider the two specific cases tested experimentally.

A.A. 1-fold anisotropy

Here we consider that the frictional coefficient is maximum in one direction along a given axis and minimum in the opposite direction along the same axis, which corresponds to $\mu(\alpha) = \mu_0\,(1 + \epsilon\,\cos\alpha)$.

In order to propose an analytical solution to the problem, we consider that the anisotropy ϵ of the friction is small. We further assume that, to the first order, the trajectory exhibits an anisotropy of the order of ϵ and search the solution in the form $r(\alpha) = r_0\,[1 + \epsilon\frac{\delta r(\alpha)}{r_0}]$. After some algebra, we get:

$$\begin{aligned} &r(\alpha) = r_0\,[1 - \epsilon'\cos(\alpha - \alpha_0)] \\ &\text{with} \quad r_0 = \sqrt{1-l^2} \quad , \quad \epsilon' = l\,\epsilon \\ &\sin\alpha_0 = l \quad \text{and} \quad \cos\alpha_0 = \sqrt{1-l^2}. \end{aligned} \tag{A.6}$$

The anisotropy ϵ' of the trajectory depends on l, thus on the length a of the link. Obviously, ϵ' vanishes for a vanishing length a. The opposite limit is that $\epsilon' \to \epsilon$ for $a \to R$ ($l \to 1$). Note also that the trajectory does not exhibit the same symmetry as the frictional coefficient. Indeed, the axis of minimum radius does not coincide with the axis of maximum frictional coefficient. Indeed, $\alpha_0 \neq \frac{\pi}{2}$ and, moreover, depends on l. The result is not surprising because the driving system is not symmetric. Note however that $\alpha_0 \to \frac{\pi}{2}$ for $a \to R$, *i.e.* when the driving system becomes almost symmetric, the link being in average perpendicular to the trajectory in this peculiar limit (The trajectory reduces to a point).

A.B. 2-fold anisotropy

Here we consider that the frictional coefficient is maximum along one axis and minimum along the perpendicular axis, which corresponds to $\mu(\alpha) = \mu_0\,(1 + \epsilon_2\,\cos 2\alpha)$.

We consider that the anisotropy of the friction is small and that, to the first order, the trajectory exhibits an anisotropy of the order of ϵ_2. We search the solution in the form $r(\alpha) = r_0\,[1 + \epsilon_2\frac{\delta r(\alpha)}{r_0}]$. After some algebra, we get:

$$\begin{aligned} &r(\alpha) = r_0\,[1 - \epsilon_2'\cos 2(\alpha - \alpha_0)] \\ &\text{with} \quad r_0 = \sqrt{R^2 - l^2} \quad , \quad \epsilon_2' = \frac{2\,l}{\sqrt{1+3\,l^2}}\,\epsilon_2 \\ &\sin 2\alpha_0 = -\frac{\sqrt{1-l^2}}{\sqrt{1+3l^2}} \quad \text{and} \quad \cos 2\alpha_0 = \frac{2\,l}{\sqrt{1+3l^2}}. \end{aligned} \tag{A.7}$$

Again, the anisotropy ϵ_2' of the trajectory depends on l. Obviously, ϵ_2' vanishes for a vanishing l. The opposite limit is that $\epsilon_2' \to \epsilon_2$ for $l \to 1$. Note also that the trajectory does not exhibit the same symmetry as the frictional coefficient. Indeed, the axis of minimum radius does not coincide with the axis of minimum frictional coefficient but, again, $\alpha_0 \to \frac{\pi}{2}$ for $l \to 1$.

[1] S. L. Bucklow, *The Description of Craquelure Patterns.* Studies in Conservation (International Institute for Conservation of Historic and Artistic Works) **42**, 129-140 (1997).

[2] S. L. Bucklow, *The Description and Classification of Craquelure.* Studies in Conservation (International Institute for Conservation of Historic and Artistic Works) **44**, 233-244 (1999).

[3] B. Cotterell, *Fracture and Life.* Imperial College Press, London (2003).

[4] A. Griffith, *The phenomena of rupture and flow* in solids. Phil. Trans. Roy. Soc. London, CCXXI-A, 163-198 (1920).

[5] B. R. Lawn and T. R. Wilshaw, *Fracture of Brittle Solids.*

Cambridge University Press, 1993.

[6] J. Leblond, *Mécanique de la rupture fragile et ductile*. Hermes Science pulication, 2003.

[7] F. Francfort, J.-J. Marigo, *Revisiting brittle fracture as an energy minimization problem*. J. Mech. Phys. Solids. **46**, 1319-1342 (1998).

[8] B. Audoly, P. Reis, and B. Roman, *Cracks in thin sheets: When geometry rules the fracture path*. Phys. Rev. Lett. **95**, 025502 (2005).

[9] A. Ghatak and L. Mahadevan, *Crack street: The cycloidalwake of a cylindertearing through a thin sheet*. Phys. Rev. Lett. **91**, 215507 (2003).

[10] P. Reis, A. N Kumar, M. D Shattuck, and B. Roman, *Unzip instabilities: Straight to oscillatory transitions in the cutting of thin polymer sheets*. Europhys. Lett. **82**, 64002 (2008).

[11] T. Wierzbicki, K.A. Trauth, and A. G. Atkins, *On diverging concertina tearing*. J. Appl. Mech. **65**, 990-997 (1998).

[12] E. Hamm, P. Reis, M. Leblanc, B.Roman, and E. Cerda, *Tearing as a test for mechanical characterization of thin adhesive films*. Nat. Mater. **7**, 386-390 (2008).

[13] A. G. Atkins, *The tear length test as an indicator of anisotropy in sheet materials*. Proc. 10th Congr. on Material Testing (Scientific Society of Mech. Engineers, Budapest), 595-600 (1991).

[14] V. Romero, *Spiraling Cracks in Thin Sheets*, PhD, Universidad de Santiago de Chile (Chile) and Université Pierre et Marie Curie (France), 2010.

[15] V. Hakim and A. Karma, *Crack path prediction in anisotropic brittle materials*. Phys. Rev. Lett. **95**, 235501 (2005).

[16] V. Hakim and A. Karma, *Laws of crack motion and phase-field models of fracture*. J. Mech. Phys. Sol. **57**, 342-368 (2009).

[17] A. Chambolle, G.A. Francfort, and J.-. Marigo, *When and how do cracks propagate?*. J. Mech. Phys. Sol. **57**, 1614-1622 (2009).

[18] A. Chambolle, F. Francfort and J.-J. Marigo, *Revisiting brittle fracture as an energy minimization problem*. J. Nonlinear Sci **20**, 395-424 (2010).

[19] G. Wulff, *On the question of speed of growth and dissolution of crystal surfaces*. Zeitsch. Kryst. Miner. **34**, 449-530 (1901).

[20] I. V. Markov, *Crystal Growth for Beginners*, 2nd Ed., World Scientific (2003).

[21] H. Kawamura, T. hatano, N. Kato, S. Biswas and B.K. Chakrabarti, *Statistical physics of fracture, friction, and earthquakes*. Rev. Mod. Phys. **84**, 839-884 (2012).

[22] K. L. Johnson, *Continuum mechanics modeling of adhesion and friction*. Langmuir **12**, 4510-4513 (1996).

[23] A Guran, F. Pfeiffer and K. Popp, Eds. *Dynamics with friction : modeling, analysis and experiment*. World Scientific (2001).

[24] C. A. Coulomb *Theorie des machines simples: en ayant égard au frottement de leurs parties et à la roideur des cordages*. Bachelier, 1821.

[25] Z. Mròz, *Contact friction models and stability problems*, in *Friction and Instabilities*, Eds J.A.C. Martins and M. Raous, CISM courses and lectures **457**, 179-232 (2002).

[26] F. Heslot *et al*, *Creep, stick-slip, and dry-friction dynamics - Experiments and a heuristic model*. Phys. Rev. E **49**, 4973-4988 (1994)

[27] C.A. Schneider, W.S. Rasband, K.W. Eliceiri, *NIH Image to ImageJ: 25 years of image analysis*. Nature Methods **9**, 671-675, (2012).